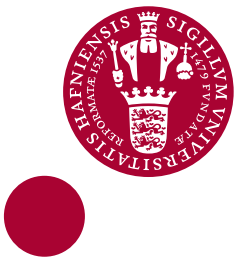

Discovery of O-glycans on atrial natriuretic peptide (ANP) that affect both its proteolytic degradation and potency at its cognate receptor

Hansen, Lasse H.; Madsen, Thomas Daugbjerg; Goth, Christoffer K.; Clausen, Henrik; Chen, Yang; Dzhoyashvili, Nina; Iyer, Seethalakshmi R.; Sangaralingham, S. Jeson; Burnett, John C.; Rehfeld, Jens F.; Vakhrushev, Sergey Y.; Schjoldager, Katrine T.; Goetze, Jens P.

Published in:
Journal of Biological Chemistry

DOI:
10.1074/jbc.RA119.008102

Publication date:
2019

Document version
Publisher's PDF, also known as Version of record

Discovery of *O*-glycans on atrial natriuretic peptide (ANP) that affect both its proteolytic degradation and potency at its cognate receptor

Received for publication, February 25, 2019, and in revised form, June 3, 2019 Published, Papers in Press, June 11, 2019, DOI 10.1074/jbc.RA119.008102

Lasse H. Hansen[‡§], Thomas Daugbjerg Madsen[§], Christoffer K. Goth[§], Henrik Clausen[§], Yang Chen[¶], Nina Dzhoyashvili[¶], Seethalakshmi R. Iyer[¶], S. Jeson Sangaralingham[¶], John C. Burnett, Jr.[¶], Jens F. Rehfeld[‡], Sergey Y. Vakhrushev[§], Katrine T. Schjoldager[§1], and Jens P. Goetze[‡‖2]

From the [‡]Copenhagen Center for Glycomics, Department of Cellular and Molecular Medicine and School of Dentistry, University of Copenhagen, 3 Blegdamsvej, 2200 Copenhagen, Denmark, the [§]Copenhagen Center for Glycomics, Department of Cellular and Molecular Medicine, School of Dentistry, University of Copenhagen, 2200 Copenhagen, Denmark, the [¶]Cardiorenal Research Laboratory, Department of Cardiovascular Medicine, Mayo Clinic, Rochester, Minnesota 55905, and the [‖]Department of Biomedical Sciences, Faculty of Health and Medical Sciences, University of Copenhagen, 3 Blegdamsvej, 2200 Copenhagen, Denmark

Edited by Gerald W. Hart

Atrial natriuretic peptide (ANP) is a peptide hormone that in response to atrial stretch is secreted from atrial myocytes into the circulation, where it stimulates vasodilatation and natriuresis. ANP is an important biomarker of heart failure where low plasma concentrations exclude cardiac dysfunction. ANP is a member of the natriuretic peptide (NP) family, which also includes the B-type natriuretic peptide (BNP) and the C-type natriuretic peptide. The proforms of these hormones undergo processing to mature peptides, and for proBNP, this process has previously been demonstrated to be regulated by *O*-glycosylation. It has been suggested that proANP also may undergo post-translational modifications. Here, we conducted a targeted *O*-glycoproteomics approach to characterize *O*-glycans on NPs and demonstrate that all NP members can carry *O*-glycans. We identified four *O*-glycosites in proANP in the porcine heart, and surprisingly, two of these were located on the mature bioactive ANP itself. We found that one of these glycans is located within a conserved sequence motif of the receptor-binding region, suggesting that *O*-glycans may serve a function beyond intracellular processing and maturation. We also identified an *O*-glycoform of proANP naturally occurring in human circulation. We demonstrated that site-specific *O*-glycosylation shields bioactive ANP from proteolytic degradation and modifies potency at its cognate receptor *in vitro*. Furthermore, we showed that ANP *O*-glycosylation attenuates acute renal and cardiovascular ANP actions *in vivo*. The discovery of novel glycosylated ANP proteoforms reported here significantly improves our understanding of cardiac endocrinology and provides important insight into the etiology of heart failure.

The natriuretic peptide (NP)[3] family comprises atrial natriuretic peptide (ANP), B-type natriuretic peptide (BNP), and C-type natriuretic peptide (CNP), which are peptide hormones involved in maintaining cardiorenal homeostasis. The cardiac NPs, ANP and BNP, possess potent diuretic and natriuretic effects as well as blood pressure-lowering properties that are mediated through the natriuretic peptide receptor A (NPR-A), whereas CNP is a potent anti-fibrotic and anti-remodeling factor acting through natriuretic peptide receptor B (NPR-B) (1–5). All three NPs are synthesized as prohormones and subsequently proteolytically activated by the proprotein convertases corin and furin to form mature receptor-binding peptide hormones. In circulation, NPs have short half-lives (*i.e.* minutes), presumably owing to processes like receptor-mediated clearance, tissue-specific metabolism, and proteolytic degradation by neprilysin and insulin-degrading enzyme. In an attempt to stabilize ANP, neprilysin inhibitors have recently been introduced for chronic heart failure treatment (6–10), and notably when neprilysin inhibition is combined with an angiotensin II receptor antagonist, cardiovascular mortality is markedly reduced (6), emphasizing the therapeutic potential of NPs in cardiovascular disease.

ProBNP is *O*-glycosylated, and *O*-glycans in close proximity to the processing site of BNP have been suggested to co-regulate processing (11). ProBNP, BNP, and the processed N-termi-

This work was supported by Rigshospitalets Forskningsraad, the Novo Nordisk Foundation, the Lundbeck Foundation, Danish National Research Foundation Grant DNRF107, and the Danish Biotechnology Center for Cellular Communication (CCC). The University of Copenhagen and Rigshospitalet have filed a patent application on part of the subject matter presented. L. H. H., T. D. M., C. K. G., S. Y. V., H. C., K. T. S., and J. P. G. are named co-inventors on the application.

This article was selected as one of our Editors' Picks.

This article contains Table S1 and Figs. S1–S5.

[1] To whom correspondence may be addressed. Tel.: 45-2992-3649; E-mail: Schjoldager@sund.ku.dk.

[2] To whom correspondence may be addressed. Tel.: 45-3545-2202; Fax: 45-3545-2880; E-mail: JPG@dadlnet.dk.

[3] The abbreviations used are: NP, natriuretic peptide; ANP, atrial natriuretic peptide; BNP, B-type natriuretic peptide; CNP, C-type natriuretic peptide; GalNAc-T, *N*-acetylgalactosaminyltransferase; PNA, peanut agglutinin; HCD, higher-energy collision dissociation; ETD, electron-transfer dissociation; Tn, GalNAcα1-*O*-Ser/Thr; T, Galβ1–3GalNAcα1-*O*-Ser/Thr; ST, NeuAcα2–3Galβ1–3GalNAcα1-*O*-Ser/Thr; diST, NeuAcα2–3Galβ1–3[NeuAcα2–6]+/-GalNAcα1-*O*-Ser/Thr; NPR-A, natriuretic peptide receptor type A; NPR-B, natriuretic peptide receptor type B; NPR-C, natriuretic peptide receptor type C; VVA, *Vicia villosa* agglutinin; pAb, polyclonal antibody; Fmoc, N-(9-fluorenyl)methoxycarbonyl; MAP, mean arterial pressure; BP, blood pressure; UV, urine output; UNaV, urinary sodium excretion; RT, room temperature; Tricine, *N*-[2-hydroxy-1,1-bis(hydroxymethyl)ethyl]glycine; PE, polyethylene; i.v., intravenous.

nal NT-proBNP are all found in circulation and serve as biomarkers for the diagnosis of heart failure. It is well-established that proBNP and NT-proBNP carry *O*-glycans of the GalNAc type (11) and that the proportion of *O*-glycosylated proBNP increases in chronic heart failure (12, 13). *O*-Glycans are known to co-regulate proprotein processing (14), and studies demonstrate that *O*-glycans in close proximity to the furin-processing site in proBNP affect activation of the peptide as well as antibody recognition (11, 14–20). It is thus believed that the *O*-glycosylation of proBNP leads to an increase in the unprocessed form in circulation and corresponding lower biological activity (16, 21). However, comprehensive studies of *O*-glycosylation of the NPs are missing. *O*-Glycosylation is the most abundant and complex regulated type of protein glycosylation, and it is estimated that >80% of proteins trafficking the secretory pathway are *O*-glycosylated (22). *O*-Glycosylation is initiated in the Golgi by a family of up to 20 polypeptide GalNAc-transferase (GalNAc-T) isoforms at serine and threonine (and possibly tyrosine) residues. The multiple GalNAc-T isoforms are differentially expressed in cells and tissues, which offers a high potential for regulation of specific *O*-glycosites. This also stresses the need to evaluate different biological sources of proteins to explore potential *O*-glycosylation (23). It is currently not possible to reliably predict *O*-glycosites, and technical analytic challenges have long hampered identification of *O*-glycosites at the proteome level (24). However, recent advances in lectin enrichment and glycoproteomics strategies have facilitated broad screening and discovery of *O*-glycosites in cells and tissues (25–28).

In this study, we performed a comprehensive glycoproteomics analysis of human plasma and mammalian tissues with known endogenous expression of NPs, using a sensitive lectin-enriched glycoproteomics strategy. We discovered novel *O*-glycans on all three NPs and surprisingly found *O*-glycans on mature NPs with two glycosites in ANP positioned in the highly conserved receptor-binding region and thus predicted to affect bioactivity. We demonstrate that *O*-glycans on mature ANP have a major impact on stability and circulation time of ANP as well as receptor activation by *in vitro* and *in vivo* studies in rats.

Results

ProANP, proBNP, and proCNP are O-glycoproteins

To explore *O*-glycans on NPs, we devised a fractionation strategy in which we extracted water-soluble proteins (*i.e.* cytosolic and secretory granular proteins) from different tissues (neonatal porcine atria, adult porcine ventricle, and human prostate cancer tissue) known to express NPs at high levels. We used a sequential enrichment strategy for *O*-glycopeptides in combination with sensitive MS-based sequencing as described previously (22, 24, 26). We predicted the most likely *O*-glycoform in cardiac tissues to be sialylated core 1 structures (ST (NeuAcα2–3Galβ1–3GalNAcα1-*O*-Ser/Thr) and/or diST (NeuAcα2–3Galβ1–3[NeuAcα2–6] GalNAcα1-*O*-Ser/Thr)). We used pretreatment of samples with neuraminidase to remove sialic acid residues to allow for efficient enrichment of core 1 glycopeptides, using peanut agglutinin (PNA) lectin weak affinity chromatography. Subsequent identification of glycosites by tandem MS was done using higher-energy collision dissociation (HCD) and/or electron-transfer dissociation (ETD) fragmentation. Identified glycopeptides were filtered to include only NPs, and 16 NP *O*-glycopeptides were identified by HCD and/or ETD fragmentation as summarized in Fig. 1*A* (Fig. S1 and Table S1). We identified both core 1 and monosialylated core 1 structures (Table S1), suggesting that the neuraminidase pretreatment was partially incomplete.

We identified *O*-glycans on all three NP members, where *O*-glycosylated proANP and proBNP were identified in porcine atrial cardiac tissues and *O*-glycosylated proCNP was identified only in human prostate cancer tissue. The NP protein sequences are conserved between humans and pigs, and all identified *O*-glycosites were within highly conserved sequence motifs between the two species (Fig. S1). Fragmentation analyses from both HCD and ETD MS/MS of tryptic *O*-glycopeptides covering proANP$_{113–126}$, proBNP$_{53–63}$, and proCNP$_{3–28}$, respectively, are shown in Fig. S2 (*A–F*). In proBNP, we confirmed the presence of two *O*-glycans at Thr^{48} and Thr^{58} (position numbers refer to proforms after signal peptide cleavage) in the propeptide (Fig. 1*B* and Fig. S2 (*C* and *D*)), both of which were previously identified in human proBNP (11, 29). In proCNP, we found a single *O*-glycan at Thr^{11} in the propeptide (Fig. S2, *E* and *F*), which we previously identified in a SimpleCell line (22). In proANP, we identified four novel *O*-glycosites with two in the propeptide at Ser$^{6/8}$ (ambiguously assigned site) and at Ser^{80}. Surprisingly, we identified two *O*-glycosites in the mature ANP at Ser^{117} and Ser^{123} (Fig. 1 (*A* and *B*), Table S1, and Fig. S2 (*A* and *B*)), and interestingly, Ser^{117} is conserved in all NPs. This represents the first *O*-glycosites in mature ANP.

Probing human ANP O-glycosites by in vitro enzyme glycosylation

We next sought to test whether particular GalNAc-T isoforms would function with ANP using *in vitro* glycosylation assays as described previously (30). Natriuretic peptides share a characteristic disulfide bridge in the C-terminal region (Cys^{105}–Cys^{121} in proANP). We used both 20-mer partly overlapping synthetic peptides covering all potential Ser/Thr acceptor residues in proANP (peptides 1–9), mature ANP with the disulfide bridge (peptide 10) (Fig. S3*A*), and a full-length recombinant proANP$_{1–126}$ protein (Fig. S3*B*). In human proANP, the four glycosites identified in porcine proANP correspond to Ser^{8} (Ser^{6} not conserved), Ser^{80}, Ser^{117}, and Ser^{123} residues, which are covered by peptides 1, 5/6, and 9/10 (Fig. S3*A*). Most of these peptides did not serve as substrates for any of the 12 tested recombinant GalNAc-T isoforms, although peptide 5, but not 6, was, albeit poorly, utilized by GalNAc-T1 (Fig. S3*A*). Interestingly, the analysis indicated two other substrate sites, Ser^{50} and Thr^{59}/Ser^{63}, in peptides 3 and 4 covering the N-terminal propeptide, which served as substrates for several GalNAc-T isoforms, including GalNAc-T1.

Next, we tested recombinant proANP$_{1–126}$ as substrate for the three most widely expressed GalNAc-T isoforms, T1, T2, and T3, and monitored incorporation of GalNAc using VVA lectin (31). In an overnight assay, we detected GalNAc incorporation by GalNAc-T1, but not by GalNAc-T2 and -T3 (Fig. S3*B*). Incorporation of GalNAc by GalNAc-T1 resulted in

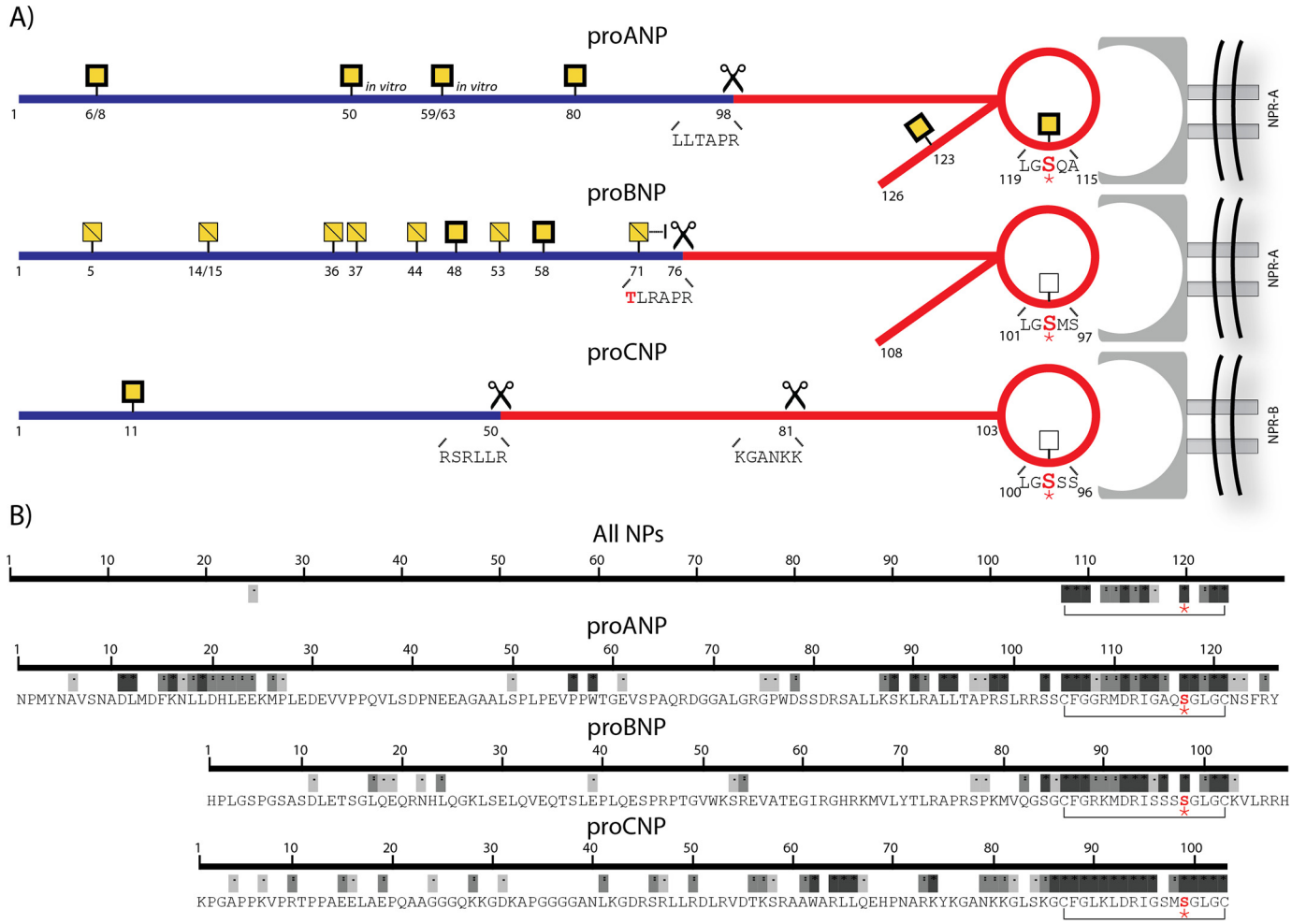

Figure 1. Summary of identified *O*-glycosites on natriuretic peptides. *A*, *schematic representation* of NPs with previously reported *O*-glycosites (*yellow squares* with *diagonal line*) and sites identified in this study (*yellow squares* with *bold*, *black frame*). The NP pro-part is shown in *blue*, and the mature bioactive hormone is shown in *red*. Receptor binding involving the cyclic part of the bioactive hormones and their cognate receptors is shown on the *right*. *Scissors* indicate corin or furin cleavage sites. A conserved serine in the mature NPs is *highlighted* in *boldface red type* and with an *asterisk* and marked with a *white box* on BNP and CNP. The six amino acids upstream of the proprotein convertase activation sites are shown with previously identified *O*-glycosites *highlighted* in *red*. *B*, analysis of NP sequence conservation. The *top panel* shows conservation among all NPs in five species. The *three bottom panels* show the conservation tracks for each NP as indicated. The conserved serine in the disulfide ring of ANP is *highlighted* in *red* and with an *asterisk*. *Dark gray*, complete conservation; *medium* and *light gray*, less conservation; *white*, no conservation. All alignments were performed in ClustalW using the NP proprotein sequences of *Homo sapiens*, *Mus musculus*, *Xenopus laevis*, *O. mykiss*, and *A. japonica*.

slower migration of both pAb proANP$_{1-16}$– and pAb proANP$_{99-126}$–immunoreactive bands corresponding to a 1–3-kDa increase in mass, suggesting that, at least *in vitro*, both proANP and N-terminal proANP$_{1-98}$ (NT-proANP) are glycosylated by GalNAc-T1.

Identification of partially O-glycosylated proANP$_{1-98}$ in human plasma

In healthy individuals, proANP forms and ANP$_{1-28}$ circulate in low picomolar ranges, which is a likely reason why these low-abundance proANP *O*-glycopeptides have not been detected in human or animal plasma in our previous *O*-glycoproteomics studies (25, 32). To search for *O*-glycosylated proANP in plasma, we therefore developed a state-of-the-art Western blotting strategy for plasma samples with high endogenous concentrations of proANP in combination with ethanol precipitation (Fig. 2*A*). We screened 20 plasma samples from our clinical routine laboratory with increased proBNP concentrations and selected the three samples with the highest proANP signal by Western blotting. We used a sensitive antibody directed to the first 16 amino acids of proANP, pAb proANP$_{1-16}$, and concluded that plasma proANP migrated as a major band around 9–10 kDa with a variable slower-migrating band at ~14 kDa (Fig. 2*A*). The prominent faster-migrating band at 9–10 kDa was concluded to correspond to NT-proANP. We speculated that the slower-migrating band at 14 kDa could represent an *O*-glycoform of proANP and explored this by treating the plasma samples with a mixture of neuraminidase and *O*-glycanase to remove core 1 *O*-glycans. This resulted in selective loss of the slower-migrating immunoreactive band in all samples (Fig. 2*A*). We further treated a pool of plasma samples with neuraminidase to remove only terminal sialic acid residues, followed by immunoprecipitation and detection using pAb proANP$_{1-16}$, and this resulted in a mobility shift of the slower migrating 14 kDa band by ~1–2 kDa (Fig. 2*B*). These results demonstrate that proANP in blood exists as

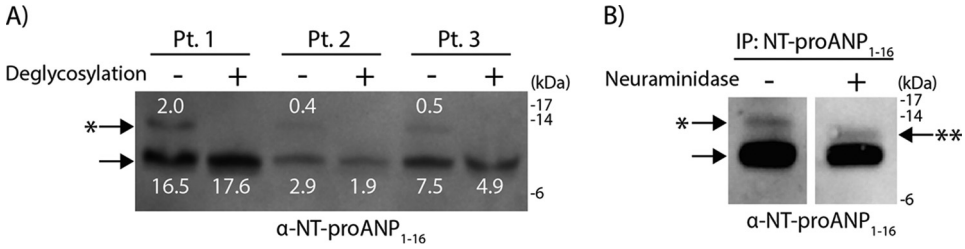

Figure 2. Identification of circulating *O*-glycosylated NT-proANP in human plasma. *A*, Western blotting with pAb proANP$_{1-16}$ of plasma from three plasma samples with high endogenous proANP concentrations subjected to deglycosylation with a broad specificity of neuraminidase and *O*-glycanase. Band intensities are shown *above* or *below* the respective bands. *B*, Western blotting with pAb proANP$_{1-16}$ of plasma treated only with neuraminidase and immunoprecipitated (*IP*) with pAb proANP$_{1-16}$. *Arrows*, 9–10 kDa bands; *arrows* with *one asterisk*, 14 kDa bands; *arrow* with *two asterisks*, 12–13 kDa band.

multiple proteoforms with a minor fraction containing sialylated core 1 *O*-glycans. Based on band intensities, we estimate that the *O*-glycoform corresponds to ~10% of total circulating proANP (Fig. 2*A*).

O-Glycosylation of ANP impacts proteolytic stability

ANP has a short half-life in circulation, ascribed to receptor-mediated uptake and degradation by neprilysin and insulin-degrading enzyme (33). Neprilysin inactivates ANP by initial cleavage between Cys^{105} and Phe^{106}, which opens the disulfide ring, and insulin-degrading enzyme inactivates ANP by initial cleavage between Ser^{123} and Phe^{124}, truncating the C terminus (34–36). *O*-Glycans in proximity of cleavage sites can modulate regulated proteolysis by, for example, proprotein convertases and ADAM metalloproteinases (14, 37), so we hypothesized that the *O*-glycans at Ser^{117} and Ser^{123} could impact degradation by neprilysin and insulin-degrading enzyme. To explore this, we used an *in vitro* proteolysis time-course assay monitoring cleavage of peptides and glycopeptides by semi-quantitative MALDI-TOF MS analysis (38).

We found that neprilysin degraded ANP completely within 15 min, whereas ANP with the simplest GalNAc (Tn) monosaccharide *O*-glycan (Tn-ANP$_{S117}$ and Tn-ANP$_{S123}$) remained at least partially intact after 60 and 15 min, respectively (Fig. 3*A*). A fraction of intact Tn-ANP$_{S117,S123}$ was still detected after a 30-min incubation. In a similar time course with insulin-degrading enzyme, ANP was completely degraded within 15 min, whereas Tn-ANP$_{S117}$ and Tn-ANP$_{S123}$ remained mainly as full-length glycopeptides after 30–60 min of incubation (Fig. 3*B*). Interestingly, Tn-ANP$_{S117,S123}$ was degraded within 15 min.

O-Glycosylation of ANP affects receptor activation

On mature ANP, the two identified glycosites, Ser^{117} and Ser^{123}, are located in the receptor-binding region and predicted to impact interaction with the atrial natriuretic peptide receptor type A (NPR-A) (Fig. 1*A*). Ser^{117} is highly conserved in all NPs, including *Xenopus laevis*, *Oncorhynchus mykiss*, and *Anguilla japonica* (Fig. 1*B*), suggesting that this site may be particularly important. To address the effect on receptor interaction, we produced a series of ANP glycopeptides corresponding to those identified by a chemoenzymatic approach (39). ANP glycopeptides with GalNAc residues at selected sites were installed by Fmoc solid-phase synthesis, and the sialylated core 1 structures were generated by stepwise enzymatic glycosylation with purified recombinant *Drosophila* core 1 synthase (*dC1GalT1*) and human α2,3-sialyltransferase (*ST3Gal1*) (Fig. 4, *A* and *B*).

To evaluate the influence of *O*-glycans on ANP activation of the cognate receptors, we used HEK293 cells stably expressing full-length coding constructs of human NPR-A or NPR-B (40). Ligand efficacy and potency were evaluated by quantifying accumulation of intracellular cGMP as a measure of receptor activation. First, we tested a panel of ANP peptides and GalNAc-glycopeptides in NPR-A (Fig. 4*B*) and NPR-B (Fig. S4), and neither of these activated NPR-B. However, whereas non-glycosylated ANP activated NPR-A within the expected EC$_{50}$ of 0.4–10 nM, the GalNAc-glycosylated ANP glycoforms with *O*-glycans at either Ser^{117} or Ser^{123} reduced the EC$_{50}$ 65–140-fold (Fig. 4, *C* and *D*), whereas the presence of *O*-glycans at both sites completely abolished receptor activation (Fig. S4*C*). To examine the effects of the elongated natural core 1 *O*-glycan structures, we tested core 1 (T), ST, and diST glycoforms, and both T-ANP$_{S117}$ and ST-ANP$_{S117}$ diminished NPR-A activation additionally 3–5-fold compared with the Tn-glycoform, whereas diST-ANP$_{S117}$ did not reach full activation even at 10 μM (Fig. 4*C*). T-ANP$_{S123}$, ST-ANP$_{S123}$, and diST-ANP$_{S123}$ diminished NPR-A activation additionally 2–6-fold compared with the Tn-glycoform (Fig. 4*D*). Elongated glycoforms of ANP$_{S123}$ tended to reach 80% efficacy, whereas ANP$_{S123}$ glycoforms reached 120% efficacy compared with ANP. Importantly, treatment of Tn-ANP$_{S117}$ with an exo-α-*N*-acetylgalactosaminidase to remove GalNAc residues (41) restored the EC$_{50}$, showing that enzymatic treatment and repurification had no effect on the functional state of ANP (Fig. S4*D*).

O-Glycosylation of ANP affects in vivo stability and activity

We further tested *in vivo* bioavailability and activity of ANP glycoforms in rats. We measured mean arterial pressure (MAP), renal actions, and peptide hormone changes *in vivo* in normal rats with 60-min intravenous infusion of synthetic ANP, ST-ANP$_{S117}$, or ST-ANP$_{S123}$, followed by 30-min post-infusion clearance. Overall, ANP induced potent blood pressure (BP)-lowering effect compared with ST-ANP$_{S117}$ or ST-ANP$_{S123}$ during infusion (Fig. 5*A*). There is a trend that MAP was sustained or further reduced by ST-ANP$_{S117}$ and ST-ANP$_{S123}$ after infusion was completed compared with the rebounding effect observed in the ANP group. Both urine output (UV) and urinary sodium excretion (UNaV) were increased by ANP infusion and not by glycosylated ANP (Fig. 5, *B* and *C*). The enhanced cardiovascular and renal actions in the ANP

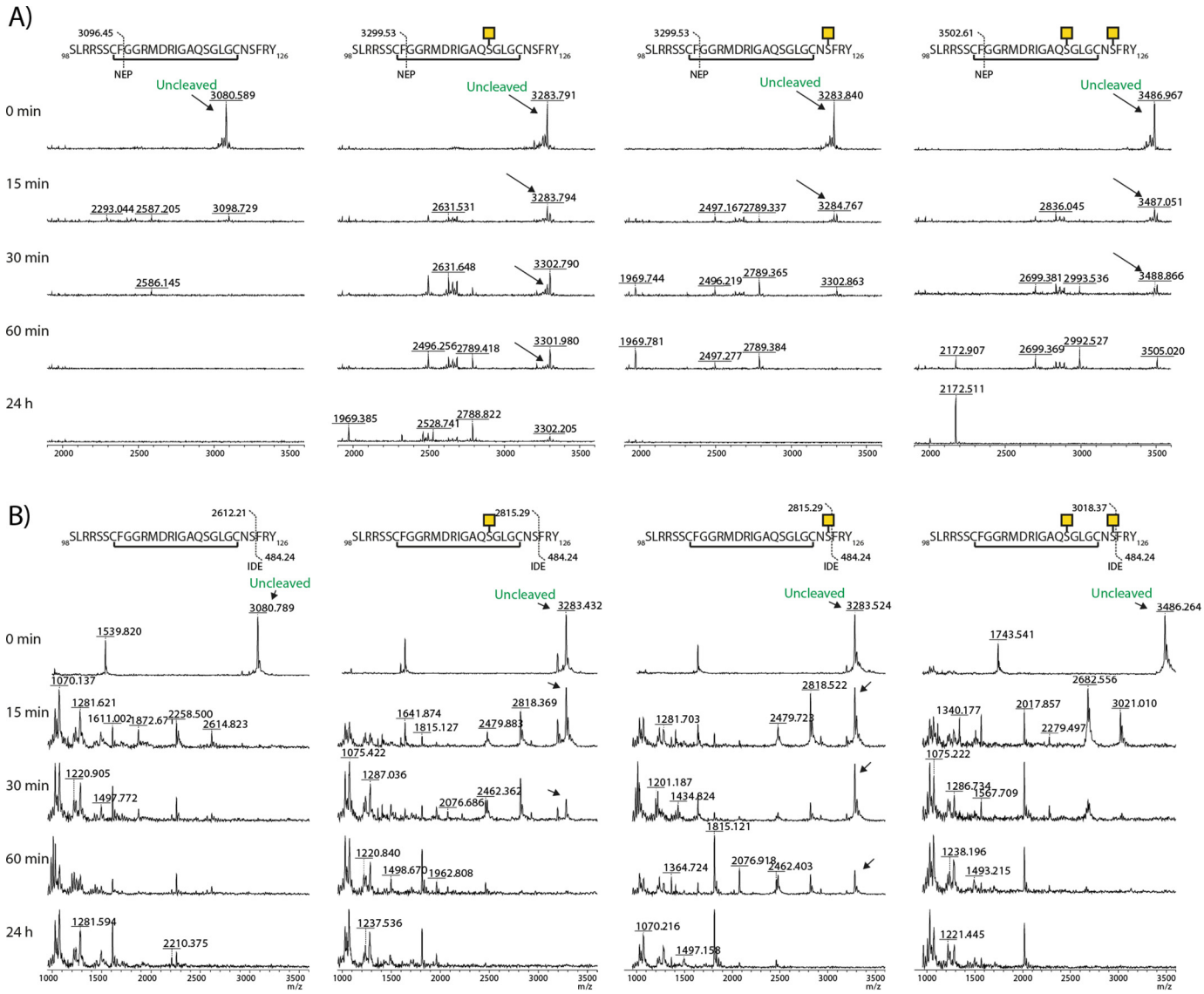

Figure 3. Proteolytic stability of ANP glycoforms. *A* and *B*, *in vitro* cleavage analysis of equal amounts of ANP and *O*-glycosylated ANP (Tn-ANP$_{S117}$, Tn-ANP$_{S123}$, or Tn-ANP$_{S117,S123}$) with either neprilysin (*A*) or insulin-degrading enzyme (*B*) in a time course up to 24 h. ANP peptide sequence with GalNAc glycosylation and initial neprilysin and insulin-degrading enzyme proteolytic cleavage sites (*vertical lines*) and their expected masses after cleavage are shown at the *top* of each *panel*. Samples were taken at the indicated time points, and the product development was monitored by MALDI-TOF MS. Intact ANP is indicated by *arrows*, and products formed by proteolytic activity have either lower or slightly higher masses. Initial cleavage by neprilysin opens the disulfide ring, which increases the mass of intact ANP with 18 Da, whereas initial cleavage by insulin-degrading enzyme leads to a loss of 466 Da. After the initial cleavage events, ANP is further degraded to products of lower masses. Assays were repeated 2–3 times with similar results, respectively. Mock treatment did not affect the ANP signal over time (not shown).

group were accompanied by significant elevation of plasma and urinary cGMP levels (Fig. S5, *A* and *B*). ST-ANP$_{S123}$ tended to increase cGMP levels as well, and ST-ANP$_{S117}$ had only a minor effect on cGMP levels. Interestingly, infusion with ST-ANP$_{S123}$ or ST-ANP$_{S117}$ presented markedly higher ANP levels in both plasma and urine compared with the ANP infusion group, indicating their exceptional stability *in vivo* (Fig. S5, *C* and *D*).

Discussion

Recent advances in *O*-glycoproteomics have provided a new perspective on the abundance of protein *O*-glycosylation and how site-specific *O*-glycosylation regulated by individual GalNAc-T isoforms serves distinct co-regulatory roles with health impact (42). Here, we performed a targeted analysis of NPs motivated partly by previous studies of BNP demonstrating a role of *O*-glycosylation in processing (16) and partly by our previous indication that antibodies to ANP were being blocked by unexplainable modifications (43). Applying a sensitive targeted glycoproteomics strategy to low-molecular weight proteins and peptides led to the discovery of *O*-glycans on all NPs and, of particular interest, the presence of *O*-glycans on the mature NPs. We demonstrated with ANP that a conserved *O*-glycosite in the receptor-binding region of NPs positively affected circulatory half-life and negatively affected NPR-A receptor activation in rats. The result adds another fundamental function to site-specific *O*-glycosylation in regulating peptide hormones (42), and this may be more generally applicable

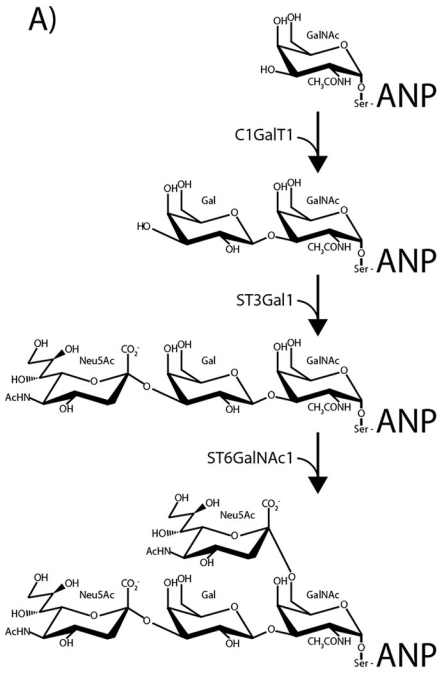

B)

Peptide name	Peptide sequence	*Modification
CNP	GLSKGCFGLKLDRIGSMSGLGC	-
ANP	SLRRSSCFGGRMDRIGAQSGLGCNSFRY	-
Tn-ANP$_{S117,S123}$	SLRRSSCFGGRMDRIGAQ*SGLGCN*SFRY	*GalNAcα1-O-Ser
Tn-ANP$_{S117}$	SLRRSSCFGGRMDRIGAQ*SGLGCNSFRY	*GalNAcα1-O-Ser
T-ANP$_{S117}$	SLRRSSCFGGRMDRIGAQ*SGLGCNSFRY	*Galβ1-3GalNAcα1-O-Ser
ST-ANP$_{S117}$	SLRRSSCFGGRMDRIGAQ*SGLGCNSFRY	*NeuAcα2-3Galβ1-3GalNAcα1-O-Ser
diST-ANP$_{S117}$	SLRRSSCFGGRMDRIGAQ*SGLGCNSFRY	*NeuAcα2-3Galβ1-3[NeuAcα2-6]GalNAcα1-O-Ser
Tn-ANP$_{S123}$	SLRRSSCFGGRMDRIGAQSGLGCN*SFRY	*GalNAcα1-O-Ser
T-ANP$_{S123}$	SLRRSSCFGGRMDRIGAQSGLGCN*SFRY	*Galβ1-3GalNAcα1-O-Ser
ST-ANP$_{S123}$	SLRRSSCFGGRMDRIGAQSGLGCN*SFRY	*NeuAcα2-3Galβ1-3GalNAcα1-O-Ser
diST-ANP$_{S123}$	SLRRSSCFGGRMDRIGAQSGLGCN*SFRY	*NeuAcα2-3Galβ1-3[NeuAcα2-6]GalNAcα1-O-Ser

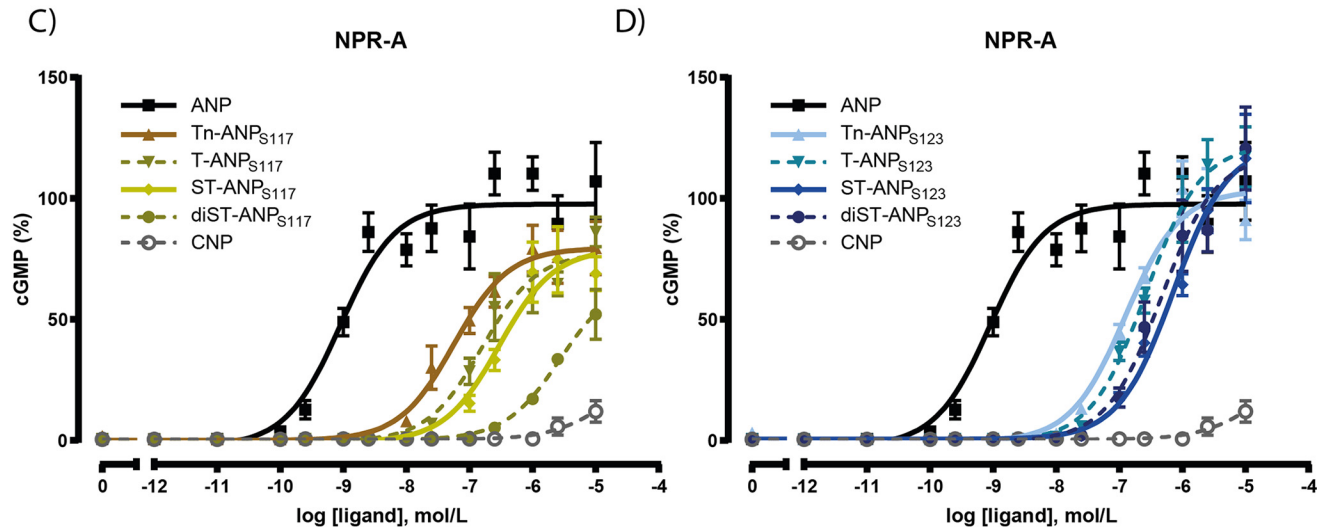

Figure 4. Analysis of natriuretic peptide receptor type A activation with ANP glycoforms. *A*, illustration of the stepwise enzymatic synthesis of ANP glycopeptides. Tn-ANP was synthesized using Fmoc solid-phase synthesis and used for further glycan elongation to produce T-ANP using *Drosophila* core 1 synthase (*dC1GalT1*), to ST-ANP using human α-2,3-sialyltransferase 1 (*ST3Gal1*), and to diST using human GalNAc α-2,6-sialyltransferase 1 (*ST6GalNAc1*). *B*, *table* summary of peptides and glycopeptides used in receptor activation assays. All peptides were synthesized with a disulfide bridge. *C*, NPR-A activation assay using ANP and glycosylated ANP variants on Ser^{117} and CNP as control. *D*, NPR-A activation assay using ANP and glycosylated ANP variants on Ser^{123} and CNP control peptide. Receptor activation was measured by an increase in cGMP content in HEK293 cells stably expressing NPR-A stimulated by increasing concentrations of peptides as indicated. The receptor activation data in *C* and *D* are directly comparable, since the experiment was performed simultaneously on the same plates. The same ANP and CNP data are shown in both *C* and *D* for purposes of clarity and ease of comparison. *Error bars*, S.E.

to short peptide hormones than currently appreciated given the general difficulties with identifying *O*-glycans.

ANP binds to NPR-A through an asymmetric interaction with the receptor homodimer, where the N-terminal part of NPR-A binds to one receptor monomer and the C-terminal part of ANP binds to the other receptor monomer (44). Thus, the entire mature ANP peptide is important for the receptor binding (45). Previous studies of ANP analogs have shown that the highly conserved Ser^{117} residue in the C-terminal loop is important for NPR-A binding, and substitution of this residue with D-Ser diminishes binding (46). In agreement with this, we found that the identified *O*-glycan at Ser^{117} in ANP decreased its activation potency with NPR-A, and this effect was exacerbated by increasing the size of the attached *O*-glycan (Fig. 4). Moreover, synthetic ANP glycoforms with *O*-glycans at both Ser^{117} and Ser^{123} completely abolished activation of NPR-A, although this glycoform with two *O*-glycans was not identified in the studied biological samples. We also explored the interaction of ANP glycoforms with the NPR-B receptor to evaluate whether *O*-glycans could affect receptor subclass selectivity, but all tested ANP glycoforms remained inactive with NPR-B similarly to unmodified ANP. We did not test for binding to NPR-C, and NPR-C has been suggested to have cardiovascular activity that goes beyond its role as a clearance receptor where

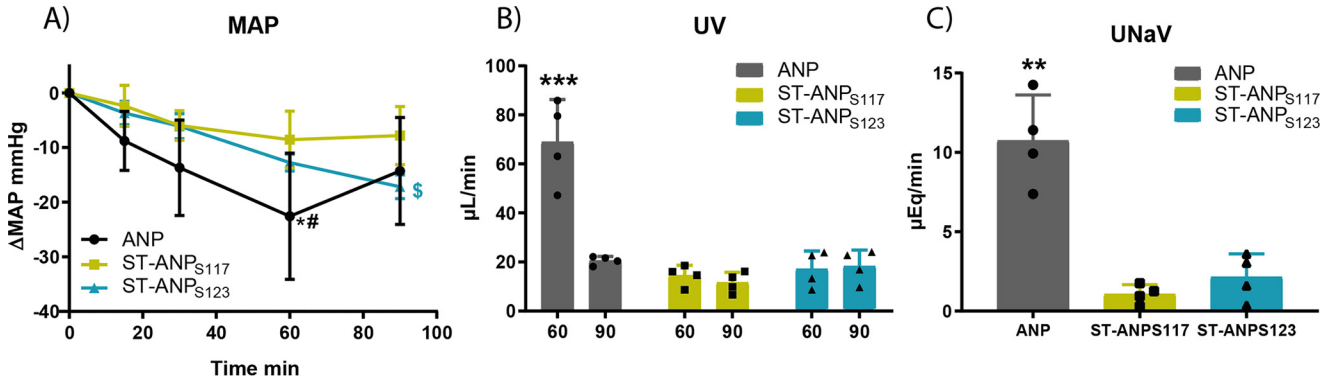

Figure 5. Acute *in vivo* actions of *O*-glycosylated ANP. ANP or *O*-glycosylated ANP with sialylated core 1 glycan on either Ser^{117} or Ser^{123} was infused into rats for 60 min followed by a post-infusion clearance period of 30 min, and mean arterial pressure (*MAP*) (*A*), urinary output (*UV*) (*B*), and urinary sodium excretion (*UNaV*) (*C*) were evaluated in the study. *, $p < 0.01$ *versus* ST-ANP$_{S117}$; #, $p < 0.05$ *versus* ST-ANP$_{S123}$; $, $p < 0.05$ *versus* ST-ANP$_{S117}$; ***, $p < 0.0001$ *versus* all groups; **, $p < 0.001$ *versus* all groups (two-way ANOVA, Tukey's post hoc tests). *Error bars*, S.D.

NPR-C activation leads to lowering of blood pressure (47–49). Future studies on the cellular biology of ANP glycoforms should include relevant primary cells or cell lines expressing endogenous natriuretic peptide receptors.

Peptide hormones, including the NPs, are rapidly degraded in circulation by neprilysin and insulin-degrading enzyme (36), and inhibitors of neprilysin increase the effects of endogenous NPs (50). The catalytic grooves of these enzymes provide for their selective specificities of the small mature forms of NPs, likely resulting from a molecular sieving function in domain 2, restricting access by larger peptides to the active site (51). *O*-Glycans are well-known to affect stability of proteins and in many cases directly co-regulate limited proteolysis (14, 37, 52), and the finding that mature ANP is stabilized by one or more *O*-glycans in *in vitro* proteolysis assays with neprilysin and insulin-degrading enzyme is in agreement with this. We further found that the proximity of the *O*-glycosites with the preferred cleavage sites of neprilysin and insulin-degrading enzyme correlated with inhibition of proteolysis (Fig. 3), and the effect of *O*-glycans on stability was confirmed in *in vivo* studies with both plasma and urine. The position and size of the *O*-glycans also affected receptor activation, and, perhaps surprisingly, the presence of a single *O*-glycan at Ser^{117} or Ser^{123} reduced, but did not abrogate, receptor activation (Fig. 4). *O*-Glycans are uniquely suited to serve fine-tuned regulatory functions because they are usually small and may be accommodated in binding interactions and because they can be differentially regulated by one of the many isoenzymes orchestrating this type of protein glycosylation, in contrast to most other types of protein glycosylation, including *N*-glycosylation (23). Further studies are needed to address the biosynthetic and genetic regulation of the identified *O*-glycans on NPs.

ANP and BNP are introduced in the clinical setting for infusion therapy for decompensated heart failure (53–55). However, several studies have failed to demonstrate improved outcome for patients, which, at least in part, appears to be because of hemodynamic effects and the induction of hypotension (56, 57). Thus, current infusion strategies are based on low-dose ANP administration over the course of several days (54). The present results suggest that introduction of *O*-glycans on these NPs could improve therapeutic use by lowering and extending receptor activation without the noted side effects. Our findings may also, at least partly, explain the "endocrine paradox" in congestive heart failure patients (58). These patients have highly increased plasma NP concentrations concomitant with edema. However, when administered recombinant BNP, they elicit natriuresis, suggesting that endogenous NPs are blunted in their bioactivity, and we hypothesize that this may be due to altered *O*-glycosylation of proBNP (15, 59). In support of this, it appears that several key glycosyltransferases involved in *O*-glycosylation initiation and elongation are up-regulated in heart failure in the left ventricle of a rat model of hypertension-induced cardiac hypertrophy (60).

In conclusion, our study suggests that all members of the NP family are naturally *O*-glycosylated and that *O*-glycans on NPs affect processing, receptor activation, and stability. We hypothesize that *O*-glycoforms of NPs are produced to fine-tune timing and functions of NPs and posit that *O*-glycosylated NPs may have potential for therapeutic use.

Materials and methods

Sample preparation and nLC-MS/MS analysis

Atrial appendage tissue from 44 newborn piglets (61), one normal porcine ventricle, and human prostate gland tissue biopsies (pooled) (62) were collected. The local ethics committee approved the use of human tissue (KF 01287197), written informed consent was obtained from all study participants, and the study abides by the Declaration of Helsinki principles. Proteins were extracted by crushing frozen tissue using a CryoPrep tissue extractor (Covaris, Woburn, MA), boiled in water for 20 min, and homogenized with an Ultra-Turrax (IKA, Staufen, Germany). After a 30-min centrifugation at 13,000 × *g*, the supernatants were collected and pooled, and protein concentration was determined using a bicinchoninic acid assay (Pierce). The prostate gland extract was then adjusted to 0.5 M CH_3COOH, precipitated by −20 °C acetone (67%), incubated for 1 h at −20 °C, and centrifuged at 16,000 × *g* for 30 min. Subsequently, the supernatant was lyophilized and reconstituted in water.

An aliquot corresponding to 3 mg of protein for the heart samples and 5 mg of protein for the prostate sample was adjusted to 50 mM ammonium bicarbonate, reduced by 5 mM DTT (30 min, 60 °C), and alkylated by adding 10 mM iodoacet-

amide (30 min, room temperature (RT)). The sample was then digested with 50 μg of trypsin (Roche Applied Science) (37 °C, overnight), purified on C18 Sep-Pak (Waters), and desialylated with 150 units of neuraminidase (P0720, New England Biolabs) in 50 mM sodium citrate (pH 6.0) (37 °C for 2 h). The digest was Sep-Pak–purified, lyophilized, and resuspended in 2 ml of PNA-binding buffer (10 mM HEPES (pH 7.4), 150 mM NaCl, 1 mM $CaCl_2$, 0.1 mM $MgCl_2$, $MnCl_2$, and $ZnCl_2$) and injected to a pre-equilibrated 2.6-m-long PNA lectin-agarose column (Vector Laboratories). The flow was set to 100 μl min^{-1}, and 1-ml fractions were collected. The sample was eluted with 3 × 1 column volume of 0.5 M galactose, 1 M galactose, and 1 M galactose, pH 3, respectively.

All samples were desalted on homemade StageTips (Empore disk-C18, 3 M) (63, 64). The acidified samples were loaded on the activated StageTips; washed with 0.1% formic acid; eluted with 50% methanol, 0.1% formic acid; lyophilized; and finally dissolved in 0.1% formic acid. Samples were analyzed on an EASY-nLC 1000 LC system (Thermo Fisher Scientific) interfaced via nanoSpray Flex ion source to an LTQ-Orbitrap Velos Pro mass spectrometer (Thermo Fisher Scientific). A precursor MS1 scan (m/z 350–1,700) of intact peptides was acquired in the Orbitrap at a nominal resolution setting of 30,000, followed by Orbitrap HCD-MS2 and ETD-MS2 (m/z of 100–2,000) of the five most abundant precursor ions in the MS1 spectrum; a minimum MS1 signal threshold of 50,000 was used for triggering data-dependent fragmentation events; and MS2 spectra were acquired at a resolution of 7,500 for HCD MS2 and 15,000 for ETD MS2. Activation times were 30 and 200 ms for HCD and ETD fragmentation, respectively; isolation width was 4 mass units, and usually 1 microscan was collected for each spectrum. Automatic gain control targets were 1,000,000 ions for Orbitrap MS1 and 100,000 for MS2 scans, and the automatic gain control for the fluoranthene ion used for ETD was 300,000. Supplemental activation (20%) of the charge-reduced species was used in the ETD analysis to improve fragmentation. Dynamic exclusion for 60 s was used to prevent repeated analysis of the same components. Polysiloxane ions at m/z 445.12003 were used as a lock mass in all runs.

Data analysis

Data processing was performed using Proteome Discoverer version 1.4 software (Thermo Fisher Scientific), using Sequest HT node as described previously with small changes (22). All spectra were initially searched with the full cleavage specificity, filtered according to the confidence level (medium, low, and unassigned), and further searched with the semi-specific enzymatic cleavage. In all cases, the precursor mass tolerance was set to 6 ppm, and fragment ion mass tolerance was set to 50 milli-mass units. Carbamidomethylation on cysteine residues was used as a fixed modification. Methionine oxidation and HexNAc and HexHexNAc, HexNAcNeuAc, and HexHexNAcNeuAc attachment to serine, threonine, and tyrosine were used as variable modifications for ETD MS2. All HCD MS2 scans were preprocessed as described (22) and searched under the same conditions mentioned above using only methionine oxidation as a variable modification. All spectra were searched against a concatenated forward/reverse *Sus scrofa* (pig)-specific database (UniProt, February 2014, containing 33,652 canonical entries) or human-specific database (UniProt, January 2013, containing 20,232 canonical entries) using a target false discovery rate of 1%. FDR was calculated using target decoy PSM validator node, a part of the Proteome Discoverer workflow. The resulting list was filtered to include only NPs with glycosylation as a modification. The full data set will be published elsewhere and made available at the GlyocDomainViewer (https://glycodomain.glycomics.ku.dk)[4] (65).

Peptide synthesis, in vitro glycosylation, and glycan elongation

Synthetic ANP and CNP peptides (Phoenix Pharmaceuticals), synthetic 20-mer ANP peptides (NeoBioLab), and ANP-Tn peptides (Synpeptide) were confirmed to elicit correct mass by MALDI-TOF analysis, and selected peptides were analyzed for purity by reverse-phase HPLC. Recombinant proANP (Immundiagnostik) was produced in *Escherichia coli*.

In vitro glycosylation of peptides was performed in 25 μl of 25 mM cacodylic acid sodium, pH 7.4, 10 mM $MnCl_2$, 0.25% Triton X-100, 4 mM UDP-GalNAc (Sigma), 10 μg of acceptor peptides, and 0.2 μg of purified recombinant glycosyltranferase enzyme. All reactions were incubated at 37 °C, and product development was evaluated by a Bruker Autoflex MALDI-TOF instrument with accompanying Compass version 1.4 FlexSeries software. Glycosylation of recombinant proANP was performed as above using 1 μg of acceptor protein and 0.6 μg of purified recombinant glycosyltransferase with complete EDTA-free protease inhibitor mixture (Roche Applied Science).

ANP-Tn peptides were elongated to T by enzymatic treatment with recombinant purified *Drosophila* core 1 synthase in 100 mM MES, 0.1% Triton X-100, 20 mM $MnCl_2$, and 0.5 mM UDP-Gal at 37 °C (39). After purification by reverse-phase HPLC (C18), the glycan was further elongated to ST by enzymatic treatment with recombinant purified α2,3-sialyltransferase in 25 mM Tris (pH 6.5) and 2 mM CMP-Neu5Ac at 37 °C and purified by reverse-phase HPLC (C18). GalNAc from Tn-ANP_{117} was removed by enzymatic treatment by exo-α-*N*-acetylgalactosaminidase (41) in 100 mM Tris (pH 7.4) and purified by reverse-phase HPLC (C18). Chemoenzymatically elongated glycopeptides and Azyme-treated Tn-ANP_{S119} were quantified by reverse-phase HPLC (C18) using ANP (≥95%, Phoenix Pharmaceuticals) as standard peptide.

Deglycosylation of plasma and Western blotting

For the human samples, the department has a general approval for using human material for analytical purposes without specific applications to the local ethics committee. All samples were anonymized prior to analyses without any possible traceability to the patient. Plasma from patients with elevated endogenous proBNP (>100 pM) was diluted 1:1 with 50 mM phosphate buffer, pH 6, and incubated with 10 milliunits of broad neuraminidase (Merck Millipore, catalogue no. 480716) and 2 milliunits of *O*-glycanase (Merck Millipore, catalogue no. 324716) for 16 h at 37 °C and subsequently precipitated by eth-

[4] Please note that the JBC is not responsible for the long-term archiving and maintenance of this site or any other third party hosted site.

anol (64%), vortexed, and centrifuged at 4,000 × *g* for 20 min at 4 °C. The pellet was discarded, and the supernatant was dried in a SpeedVac and resuspended in water. For specific removal of sialic acids, the sample was treated with 100 units of α2–3,6,8-neuraminidase (New England Biolabs) for 1 h at 37 °C on 330 μl of supernatant in a total volume of 1 ml in 50 mM sodium acetate, pH 5. For immunoprecipitation, samples were precipitated with rabbit pAb NT-proANP$_{1-16}$ (66) using Dynabeads protein A (Thermo Fisher Scientific) according to the manufacturer's instructions.

All samples were run on 16%/10%/6% Tris-Tricine gels at 125 V for 90 min and transferred to nitrocellulose membranes, and nonspecific binding was blocked using 5% skim milk in TBST. The blocked membranes were incubated with primary antibody pAb NT-proANP$_{1-16}$ or pAb proANP$_{99-126}$ diluted 1:1,000 overnight at 4 °C followed by secondary antibody goat anti-rabbit IgG coupled to horseradish peroxidase (Cell Signaling) diluted 1:2,000 for 1 h at RT. For lectin blots, 1% polyvinylpyrrolidone was used as blocking reagent, and lectin used was VVA-biotin (Vector Laboratories) diluted 1:2,000 overnight at 4 °C followed by secondary antibody streptavidin coupled to horseradish peroxidase (Dako, Agilent) diluted 1:4,000 for 1 h at RT. For development, SuperSignal West Pico Chemiluminescent Substrate (Thermo Scientific) was used on an Odyssey Fc Imaging System (LI-COR Biosciences). Band intensities were calculated using Image Studio version 2.0.38 (LI-COR Biosciences) and are shown as signal/area × 10^5.

ANP receptor cGMP activation assay

The cGMP content in HEK293 cells stimulated with peptide was measured using the cGMP kit (Cisbio) according to the manufacturer's instructions. Briefly, HEK293 cells stably expressing either human NPR-A or human NPR-B (40) were resuspended in Dulbecco's modified Eagle's medium buffer supplemented with 25 mM HEPES, pH 7.4, 0.1% BSA, and 1 mM 3-isobutyl-1-methylxanthine (Sigma) to achieve a cell density of 0.4 million cells/ml. Stimulated cells (2,000 cells/well) were incubated at 37 °C for 30 min before the cells were lysed, anti-cGMP cryptate conjugate and cGMP-d_2 conjugate were added, and the plate was incubated for 1 h at room temperature. The plate was read on an Enspire Multilabel Reader (PerkinElmer Life Sciences) with excitation at 340 nm and measurements of emission at 615 and 665 nm. The FRET ratios (665/615 nm) were converted into cGMP concentrations by interpolating values from a cGMP standard curve.

Proteolytic degradation assay

In vitro cleavage activity was assayed by adding 1 ng of neprilysin (R&D Systems) or 50 ng of insulin-degrading enzyme (R&D Systems) to 325 pmol of peptide or glycopeptide substrate in a total volume of 10 μl. Reactions were performed in 50 mM Tris, 0.05% Brij-35, pH 9 (neprilysin), or 50 mM Tris, 20 mM NaCl, pH 7.5 (insulin-degrading enzyme), and incubated at 37 °C. Product development was monitored after 15 min, 30 min, 60 min, and 24 h by MALDI-TOF analysis.

In vivo evaluation of glycosylated ANP

We investigated the BP actions of equimolar doses of (600 pmol/kg/min) ANP, ST-ANP$_{S117}$, or ST-ANP$_{S123}$ (n = 4/group) in normal male Sprague–Dawley rats (250–350 g; Charles River Laboratories, Wilmington, MA). Studies were performed in accordance with the Animal Welfare Act and with approval of the Mayo Clinic Institutional Animal Care and Use Committee.

Anesthesia in rats was induced with 133 mg/kg intraperitoneal inactin (Sigma), and rats were maintained on a heating pad for 1 h until complete anesthesia was achieved. With oxygen flow, the rats were then subjected to catherizations and blood and urine collections (2). A polyethylene (PE)-50 tube catheter was placed into the jugular vein for intravenous (i.v.) saline and peptide infusion. The carotid artery was cannulated with a PE-50 tube catheter for BP measurement (Sonometrics, London, Canada). After completion of the above procedural setup, a 45-min equilibration period was performed, which included continuous i.v. saline infusion. After the 45-min equilibration period, baseline (0 min) BP was recorded. The inulin and saline infusion was replaced by continuous i.v. infusion of either ANP, ST-ANP$_{S117}$, or ST-ANP$_{S123}$ for 60 min. The infusion rate was weight-adjusted and equals the weight × 0.7/6,000 ml/min. A post-infusion clearance (time 60–90 min) was performed for 30 min. At the end of the study, blood was collected to determine plasma ANP and cGMP levels by radioimmunoassay and ELISA. Glycosylation on Ser-117 of ANP underestimates the actual ST-ANP$_{S117}$ concentration (data not shown). Urine was collected at the end of the infusion and post-infusion clearances (time = 60 and 90 min). Urinary sodium was measured with pHOx Ultra (Nova Biomedical, Waltham, MA). UV and UNaV were calculated as urine volume or sodium clearance per min. Urinary cGMP and ANP excretion rate were calculated based on raw concentrations obtained in the urine and UV.

Statistical analysis

In vitro receptor activation data are represented as mean ± S.E. *In vivo* data are represented as mean ± S.D. One-way ANOVA was used for comparison of more than two groups, followed by Tukey's post hoc tests, and two-way ANOVA was used when multiple time points were involved. Unpaired t test was used for comparison of two groups. Statistical significance is defined as $p < 0.05$ (two-tailed). Data were analyzed with GraphPad Prism version 8 software.

Author contributions—L. H. H., T. D. M., C. K. G., H. C., J. C. B., K. T. S., and J. P. G. conceptualization; L. H. H., Y. C., N. D., S. R. I., S. J. S., and S. Y. V. data curation; L. H. H., T. D. M., C. K. G., Y. C., and S. Y. V. formal analysis; L. H. H. validation; L. H. H., T. D. M., Y. C., N. D., and J. C. B. investigation; L. H. H., T. D. M., C. K. G., Y. C., N. D., S. R. I., S. J. S., J. C. B., S. Y. V., K. T. S., and J. P. G. methodology; L. H. H. writing-original draft; L. H. H., H. C., K. T. S., and J. P. G. project administration; L. H. H., T. D. M., C. K. G., H. C., Y. C., N. D., S. R. I., S. J. S., J. C. B., J. F. R., S. Y. V., K. T. S., and J. P. G. writing-review and editing; H. C., Y. C., J. C. B., J. F. R., K. T. S., and J. P. G. resources; H. C., J. F. R., K. T. S., and J. P. G. supervision; J. C. B., K. T. S., and J. P. G. funding acquisition.

Acknowledgments—We are grateful for the tissue samples kindly provided by Julie Smith and Søren Junge Nielsen and for the expert technical assistance by Dijana Terzic and Anne Asanovski. Moreover, we thank personal assistant Connie Bundgaard for help with formatting the manuscript.

References

1. Nielsen, S. J., Gøtze, J. P., Jensen, H. L., and Rehfeld, J. F. (2008) ProCNP and CNP are expressed primarily in male genital organs. *Regul. Pept.* **146,** 204–212 CrossRef Medline
2. Chen, Y., Zheng, Y., Iyer, S. R., Harders, G. E., Pan, S., Chen, H. H., Ichiki, T., Burnett, J. C., Jr., and Sangaralingham, S. J. (2019) C53: a novel particulate guanylyl cyclase B receptor activator that has sustained activity *in vivo* with anti-fibrotic actions in human cardiac and renal fibroblasts. *J. Mol. Cell. Cardiol.* **130,** 140–150 CrossRef Medline
3. Moyes, A. J., Chu, S. M., Aubdool, A. A., Dukinfield, M. S., Margulies, K. B., Bedi, K. C., Hodivala-Dilke, K., Baliga, R. S., and Hobbs, A. J. (2019) C-type natriuretic peptide co-ordinates cardiac structure and function. *Eur. Heart J.* 10.1093/eurheartj/ehz093 CrossRef Medline
4. Yip, C. Y. Y., Blaser, M. C., Mirzaei, Z., Zhong, X., and Simmons, C. A. (2011) Inhibition of pathological differentiation of valvular interstitial cells by C-type natriuretic peptide. *Arterioscler. Thromb. Vasc. Biol.* **31,** 1881–1889 CrossRef Medline
5. Soeki, T., Kishimoto, I., Okumura, H., Tokudome, T., Horio, T., Mori, K., and Kangawa, K. (2005) C-type natriuretic peptide, a novel antifibrotic and antihypertrophic agent, prevents cardiac remodeling after myocardial infarction. *J. Am. Coll. Cardiol.* **45,** 608–616 CrossRef Medline
6. McMurray, J. J. V., Packer, M., Desai, A. S., Gong, J., Lefkowitz, M. P., Rizkala, A. R., Rouleau, J. L., Shi, V. C., Solomon, S. D., Swedberg, K., Zile, M. R., and PARADIGM-HF Investigators and Committees (2014) Angiotensin–neprilysin inhibition *versus* enalapril in heart failure. *N. Engl. J. Med.* **371,** 993–1004 CrossRef Medline
7. Kostis, J. B., Packer, M., Black, H. R., Schmieder, R., Henry, D., and Levy, E. (2004) Omapatrilat and enalapril in patients with hypertension: the omapatrilat cardiovascular treatment *vs.* enalapril (OCTAVE) trial. *Am. J. Hypertens.* **17,** 103–111 CrossRef Medline
8. Packer, M., Califf, R. M., Konstam, M. A., Krum, H., McMurray, J. J., Rouleau, J. L., and Swedberg, K. (2002) Comparison of omapatrilat and enalapril in patients with chronic heart failure: the omapatrilat *versus* enalapril randomized trial of utility in reducing events (OVERTURE). *Circulation* **106,** 920–926 CrossRef Medline
9. Ruilope, L. M., Dukat, A., Böhm, M., Lacourcière, Y., Gong, J., and Lefkowitz, M. P. (2010) Blood-pressure reduction with LCZ696, a novel dual-acting inhibitor of the angiotensin II receptor and neprilysin: a randomised, double-blind, placebo-controlled, active comparator study. *Lancet* **375,** 1255–1266 CrossRef Medline
10. Solomon, S. D., Zile, M., Pieske, B., Voors, A., Shah, A., Kraigher-Krainer, E., Shi, V., Bransford, T., Takeuchi, M., Gong, J., Lefkowitz, M., Packer, M., McMurray, J. J., and Prospective comparison of ARNI with ARB on Management Of heart failUre with preserved ejectioN fracTion (PARAMOUNT) Investigators (2012) The angiotensin receptor neprilysin inhibitor LCZ696 in heart failure with preserved ejection fraction: a phase 2 double-blind randomised controlled trial. *Lancet* **380,** 1387–1395 CrossRef Medline
11. Schellenberger, U., O'Rear, J., Guzzetta, A., Jue, R. A., Protter, A. A., and Pollitt, N. S. (2006) The precursor to B-type natriuretic peptide is an *O*-linked glycoprotein. *Arch. Biochem. Biophys.* **451,** 160–166 CrossRef Medline
12. Costello-Boerrigter, L. C., Lapp, H., Boerrigter, G., Lerman, A., Bufe, A., Macheret, F., Heublein, D. M., Larue, C., and Burnett, J. C. (2013) Secretion of prohormone of B-type natriuretic peptide, proBNP1–108, is increased in heart failure. *JACC Heart Fail.* **1,** 207–212 CrossRef Medline
13. Nakagawa, Y., Nishikimi, T., Kuwahara, K., Fujishima, A., Oka, S., Tsutamoto, T., Kinoshita, H., Nakao, K., Cho, K., Inazumi, H., Okamoto, H., Nishida, M., Kato, T., Fukushima, H., Yamashita, J. K., *et al.* (2017) MiR30-GALNT1/2 axis-mediated glycosylation contributes to the increased secretion of inactive human prohormone for brain natriuretic peptide (proBNP) from failing hearts. *J. Am. Heart Assoc.* **6,** e003601 CrossRef Medline
14. Schjoldager, K. T.-B. G., Vester-Christensen, M. B., Goth, C. K., Petersen, T. N., Brunak, S., Bennett, E. P., Levery, S. B., and Clausen, H. (2011) A systematic study of site-specific GalNAc-type *O*-glycosylation modulating proprotein convertase processing. *J. Biol. Chem.* **286,** 40122–40132 CrossRef Medline
15. Vodovar, N., Séronde, M.-F., Laribi, S., Gayat, E., Lassus, J., Boukef, R., Nouira, S., Manivet, P., Samuel, J.-L., Logeart, D., Ishihara, S., Cohen Solal, A., Januzzi, J. L., Richards, A. M., Launay, J.-M., Mebazaa, A., and GREAT Network (2014) Post-translational modifications enhance NT-proBNP and BNP production in acute decompensated heart failure. *Eur. Heart J.* **35,** 3434–3441 CrossRef Medline
16. Semenov, A. G., Postnikov, A. B., Tamm, N. N., Seferian, K. R., Karpova, N. S., Bloshchitsyna, M. N., Koshkina, E. V., Krasnoselsky, M. I., Serebryanaya, D. V., and Katrukha, A. G. (2009) Processing of pro-brain natriuretic peptide is suppressed by *O*-glycosylation in the region close to the cleavage site. *Clin. Chem.* **55,** 489–498 CrossRef Medline
17. Peng, J., Jiang, J., Wang, W., Qi, X., Sun, X.-L., and Wu, Q. (2011) Glycosylation and processing of pro-B-type natriuretic peptide in cardiomyocytes. *Biochem. Biophys. Res. Commun.* **411,** 593–598 CrossRef Medline
18. Tonne, J. M., Campbell, J. M., Cataliotti, A., Ohmine, S., Thatava, T., Sakuma, T., Macheret, F., Huntley, B. K., Burnett, J. C., Jr., and Ikeda, Y. (2011) Secretion of glycosylated pro-B-type natriuretic peptide from normal cardiomyocytes. *Clin. Chem.* **57,** 864–873 CrossRef Medline
19. Goetze, J. P. (2012) B-type natriuretic peptide: from posttranslational processing to clinical measurement. *Clin. Chem.* **58,** 83–91 CrossRef Medline
20. Zois, N. E., Bartels, E. D., Hunter, I., Kousholt, B. S., Olsen, L. H., and Goetze, J. P. (2014) Natriuretic peptides in cardiometabolic regulation and disease. *Nat. Rev. Cardiol.* **11,** 403–412 CrossRef Medline
21. Nishikimi, T., Okamoto, H., Nakamura, M., Ogawa, N., Horii, K., Nagata, K., Nakagawa, Y., Kinoshita, H., Yamada, C., Nakao, K., Minami, T., Kuwabara, Y., Kuwahara, K., Masuda, I., Kangawa, K., Minamino, N., and Nakao, K. (2013) Direct immunochemiluminescent assay for proBNP and total BNP in human plasma proBNP and total BNP levels in normal and heart failure. *PLoS One* **8,** e53233 CrossRef Medline
22. Steentoft, C., Vakhrushev, S. Y., Joshi, H. J., Kong, Y., Vester-Christensen, M. B., Schjoldager, K. T.-B. G., Lavrsen, K., Dabelsteen, S., Pedersen, N. B., Marcos-Silva, L., Gupta, R., Bennett, E. P., Mandel, U., Brunak, S., Wandall, H. H., *et al.* (2013) Precision mapping of the human *O*-GalNAc glycoproteome through SimpleCell technology. *EMBO J.* **32,** 1478–1488 CrossRef Medline
23. Bennett, E. P., Mandel, U., Clausen, H., Gerken, T. A., Fritz, T. A., and Tabak, L. A. (2012) Control of mucin-type *O*-glycosylation: a classification of the polypeptide GalNAc-transferase gene family. *Glycobiology* **22,** 736–756 CrossRef Medline
24. Levery, S. B., Steentoft, C., Halim, A., Narimatsu, Y., Clausen, H., and Vakhrushev, S. Y. (2015) Advances in mass spectrometry driven *O*-glycoproteomics. *Biochim. Biophys. Acta* **1850,** 33–42 CrossRef Medline
25. King, S. L., Joshi, H. J., Schjoldager, K. T., Halim, A., Madsen, T. D., Dziegiel, M. H., Woetmann, A., Vakhrushev, S. Y., and Wandall, H. H. (2017) Characterizing the *O*-glycosylation landscape of human plasma, platelets, and endothelial cells. *Blood Adv.* **1,** 429–442 CrossRef Medline
26. Khetarpal, S. A., Schjoldager, K. T., Christoffersen, C., Raghavan, A., Edmondson, A. C., Reutter, H. M., Ahmed, B., Ouazzani, R., Peloso, G. M., Vitali, C., Zhao, W., Somasundara, A. V. H., Millar, J. S., Park, Y. S., Fernando, G., *et al.* (2016) Loss of function of GALNT2 lowers high-density lipoproteins in humans, nonhuman primates, and rodents. *Cell Metab.* **24,** 234–245 CrossRef Medline
27. Hintze, J., Ye, Z., Narimatsu, Y., Madsen, T. D., Joshi, H. J., Goth, C. K., Linstedt, A., Bachert, C., Mandel, U., Bennett, E. P., Vakhrushev, S. Y., and Schjoldager, K. T. (2018) Probing the contribution of individual polypeptide GalNAc-transferase isoforms to the *O*-glycoproteome by inducible expression in isogenic cell lines. *J. Biol. Chem.* **293,** 19064–19077 CrossRef Medline

28. Yang, W., Ao, M., Hu, Y., Li, Q. K., and Zhang, H. (2018) Mapping the *O*-glycoproteome using site-specific extraction of *O*-linked glycopeptides (EXoO). *Mol. Syst. Biol.* **14,** e8486 CrossRef Medline
29. Halfinger, B., Hammerer-Lercher, A., Amplatz, B., Sarg, B., Kremser, L., and Lindner, H. H. (2017) Unraveling the molecular complexity of *o*-glycosylated endogenous (N-terminal) pro-B-type natriuretic peptide forms in blood plasma of patients with severe heart failure. *Clin. Chem.* **63,** 359–368 CrossRef Medline
30. Kong, Y., Joshi, H. J., Schjoldager, K. T. B. G., Madsen, T. D., Gerken, T. A., Vester-Christensen, M. B., Wandall, H. H., Bennett, E. P., Levery, S. B., Vakhrushev, S. Y., and Clausen, H. (2015) Probing polypeptide GalNAc-transferase isoform substrate specificities by *in vitro* analysis. *Glycobiology* **25,** 55–65 CrossRef Medline
31. Pedersen, N. B., Wang, S., Narimatsu, Y., Yang, Z., Halim, A., Schjoldager, K. T.-B. G., Madsen, T. D., Seidah, N. G., Bennett, E. P., Levery, S. B., and Clausen, H. (2014) Low density lipoprotein receptor class a repeats are *o*-glycosylated in linker regions. *J. Biol. Chem.* **289,** 17312–17324 CrossRef Medline
32. Schjoldager, K. T., Joshi, H. J., Kong, Y., Goth, C. K., King, S. L., Wandall, H. H., Bennett, E. P., Vakhrushev, S. Y., and Clausen, H. (2015) Deconstruction of *O*-glycosylation–GalNAc-T isoforms direct distinct subsets of the *O*-glycoproteome. *EMBO Rep.* **16,** 1713–1722 CrossRef Medline
33. Yandle, T. G., Richards, A. M., Nicholls, M. G., Cuneo, R., Espiner, E. A., and Livesey, J. H. (1986) Metabolic clearance rate and plasma half life of α-human atrial natriuretic peptide in man. *Life Sci.* **38,** 1827–1833 CrossRef Medline
34. Vanneste, Y., Michel, A., Dimaline, R., Najdovski, T., and Deschodt-Lanckman, M. (1988) Hydrolysis of α-human atrial natriuretic peptide *in vitro* by human kidney membranes and purified endopeptidase-24.11. Evidence for a novel cleavage site. *Biochem. J.* **254,** 531–537 CrossRef Medline
35. Johnson, G. R., Arik, L., and Foster, C. J. (1989) Metabolism of ^{125}I-atrial natriuretic factor by vascular smooth muscle cells: evidence for a peptidase that specifically removes the COOH-terminal tripeptide. *J. Biol. Chem.* **264,** 11637–11642 Medline
36. Potter, L. R. (2011) Natriuretic peptide metabolism, clearance and degradation. *FEBS J.* **278,** 1808–1817 CrossRef Medline
37. Goth, C. K., Halim, A., Khetarpal, S. A., Rader, D. J., Clausen, H., and Schjoldager, K. T.-B. G. (2015) A systematic study of modulation of ADAM-mediated ectodomain shedding by site-specific *O*-glycosylation. *Proc. Natl. Acad. Sci. U.S.A.* **112,** 14623–14628 CrossRef Medline
38. Kato, K., Jeanneau, C., Tarp, M. A., Benet-Pagès, A., Lorenz-Depiereux, B., Bennett, E. P., Mandel, U., Strom, T. M., and Clausen, H. (2006) Polypeptide GalNAc-transferase T3 and familial tumoral calcinosis: secretion of fibroblast growth factor 23 requires *O*-glycosylation. *J. Biol. Chem.* **281,** 18370–18377 CrossRef Medline
39. Tarp, M. A., Sørensen, A. L., Mandel, U., Paulsen, H., Burchell, J., Taylor-Papadimitriou, J., and Clausen, H. (2007) Identification of a novel cancer-specific immunodominant glycopeptide epitope in the MUC1 tandem repeat. *Glycobiology* **17,** 197–209 CrossRef Medline
40. Dickey, D. M., Burnett, J. C., Jr., and Potter, L. R. (2008) Novel bifunctional natriuretic peptides as potential therapeutics. *J. Biol. Chem.* **283,** 35003–35009 CrossRef Medline
41. Liu, Q. P., Sulzenbacher, G., Yuan, H., Bennett, E. P., Pietz, G., Saunders, K., Spence, J., Nudelman, E., Levery, S. B., White, T., Neveu, J. M., Lane, W. S., Bourne, Y., Olsson, M. L., *et al.* (2007) Bacterial glycosidases for the production of universal red blood cells. *Nat. Biotechnol.* **25,** 454–464 CrossRef Medline
42. Goth, C. K., Vakhrushev, S. Y., Joshi, H. J., Clausen, H., and Schjoldager, K. T. (2018) Fine-tuning limited proteolysis: a major role for regulated site-specific *O*-glycosylation. *Trends Biochem. Sci.* **43,** 269–284 CrossRef Medline
43. Hunter, I., Alehagen, U., Dahlström, U., Rehfeld, J. F., Crimmins, D. L., and Goetze, J. P. (2011) N-terminal pro-atrial natriuretic peptide measurement in plasma suggests covalent modification. *Clin. Chem.* **57,** 1327–1330 CrossRef Medline
44. Ogawa, H., Qiu, Y., Ogata, C. M., and Misono, K. S. (2004) Crystal structure of hormone-bound atrial natriuretic peptide receptor extracellular domain. *J. Biol. Chem.* **279,** 28625–28631 CrossRef Medline
45. Bovy, P. R., O'Neal, J. M., Olins, G. M., and Patton, D. R. (1989) Identification of structural requirements for analogues of atrial natriuretic peptide (ANP) to discriminate between ANP receptor subtypes. *J. Med. Chem.* **32,** 869–874 CrossRef Medline
46. Scarborough, R. M., McEnroe, G. A., Arfsten, A., Kang, L. L., Schwartz, K., and Lewicki, J. A. (1988) D-Amino acid-substituted atrial natriuretic peptide analogs reveal novel receptor recognition requirements. *J. Biol. Chem.* **263,** 16818–16822 Medline
47. Ren, M., Ng, F. L., Warren, H. R., Witkowska, K., Baron, M., Jia, Z., Cabrera, C., Zhang, R., Mifsud, B., Munroe, P. B., Xiao, Q., Townsend-Nicholson, A., Hobbs, A. J., Ye, S., and Caulfield, M. J. (2018) The biological impact of blood pressure-associated genetic variants in the natriuretic peptide receptor C gene on human vascular smooth muscle. *Hum. Mol. Genet.* **27,** 199–210 CrossRef Medline
48. Moyes, A. J., Khambata, R. S., Villar, I., Bubb, K. J., Baliga, R. S., Lumsden, N. G., Xiao, F., Gane, P. J., Rebstock, A. S., Worthington, R. J., Simone, M. I., Mota, F., Rivilla, F., Vallejo, S., Peiró, C., Sánchez Ferrer, C. F., Djordjevic, S., Caulfield, M. J., MacAllister, R. J., Selwood, D. L., Ahluwalia, A., and Hobbs, A. J. (2014) Endothelial C-type natriuretic peptide maintains vascular homeostasis. *J. Clin. Invest.* **124,** 4039–4051 CrossRef Medline
49. Li, Y., Sarkar, O., Brochu, M., and Anand-Srivastava, M. B. (2014) Natriuretic peptide receptor-C attenuates hypertension in spontaneously hypertensive rats: role of nitroxidative stress and G_i proteins. *Hypertension.* **63,** 846–855 CrossRef Medline
50. Charles, C. J., Espiner, E. A., Nicholls, M. G., Richards, A. M., Yandle, T. G., Protter, A., and Kosoglou, T. (1996) Clearance receptors and endopeptidase 24.11: equal role in natriuretic peptide metabolism in conscious sheep. *Am. J. Physiol.* **271,** R373–R380 Medline
51. Oefner, C., D'Arcy, A., Hennig, M., Winkler, F. K., and Dale, G. E. (2000) Structure of human neutral endopeptidase (neprilysin) complexed with phosphoramidon. *J. Mol. Biol.* **296,** 341–349 CrossRef Medline
52. Schjoldager, K. T.-B. G., and Clausen, H. (2012) Site-specific protein *O*-glycosylation modulates proprotein processing: deciphering specific functions of the large polypeptide GalNAc-transferase gene family. *Biochim. Biophys. Acta* **1820,** 2079–2094 CrossRef Medline
53. Boerrigter, G., and Burnett, J. C. (2011) Natriuretic peptides renal protective after all? *J. Am. Coll. Cardiol.* **58,** 904–906 CrossRef Medline
54. Hata, N., Seino, Y., Tsutamoto, T., Hiramitsu, S., Kaneko, N., Yoshikawa, T., Yokoyama, H., Tanaka, K., Mizuno, K., Nejima, J., and Kinoshita, M. (2008) Effects of carperitide on the long-term prognosis of patients with acute decompensated chronic heart failure: the PROTECT multicenter randomized controlled study. *Circ. J.* **72,** 1787–1793 CrossRef Medline
55. van Deursen, V. M., Hernandez, A. F., Stebbins, A., Hasselblad, V., Ezekowitz, J. A., Califf, R. M., Gottlieb, S. S., O'Connor, C. M., Starling, R. C., Tang, W. H. W., McMurray, J. J., Dickstein, K., and Voors, A. A. (2014) Nesiritide, renal function, and associated outcomes during hospitalization for acute decompensated heart failure: results from the Acute Study of Clinical Effectiveness of Nesiritide and Decompensated Heart Failure (ASCEND-HF). *Circulation* **130,** 958–965 CrossRef Medline
56. Topol, E. J. (2005) Nesiritide - not verified. *N. Engl. J. Med.* **353,** 113–116 CrossRef Medline
57. Topol, E. J. (2011) The lost decade of nesiritide. *N. Engl. J. Med.* **365,** 81–82 CrossRef Medline
58. Goetze, J. P., Kastrup, J., and Rehfeld, J. F. (2003) The paradox of increased natriuretic hormones in congestive heart failure patients: does the endocrine heart also fail in heart failure? *Eur. Heart J.* **24,** 1471–1472 CrossRef Medline
59. Ichiki, T., and Burnett, J. C. (2014) Post-transcriptional modification of pro-BNP in heart failure: is glycosylation and circulating furin key for cardiovascular homeostasis? *Eur. Heart J.* **35,** 3001–3003 CrossRef Medline
60. Nagai-Okatani, C., and Minamino, N. (2016) Aberrant glycosylation in the left ventricle and plasma of rats with cardiac hypertrophy and heart failure. *PLoS One* **11,** e0150210 CrossRef Medline
61. Smith, J., Christoffersen, C., Nørgaard, L. M., Olsen, L. H., Vejlstrup, N. G., Andersen, C. B., and Goetze, J. P. (2013) Cardiac natriuretic peptide gene

expression and plasma concentrations during the first 72 hours of life in piglets. *Endocrinology* **154,** 1864–1872 CrossRef Medline
62. Nielsen, S. J., Iversen, P., Rehfeld, J. F., Jensen, H. L., and Goetze, J. P. (2009) C-type natriuretic peptide in prostate cancer. *APMIS* **117,** 60–67 CrossRef Medline
63. Bagdonaite, I., Nordén, R., Joshi, H. J., King, S. L., Vakhrushev, S. Y., Olofsson, S., and Wandall, H. H. (2016) Global mapping of *O*-glycosylation of varicella zoster virus, human cytomegalovirus, and Epstein-Barr virus. *J. Biol. Chem.* **291,** 12014–12028 CrossRef Medline
64. Larsen, I. S. B., Narimatsu, Y., Joshi, H. J., Yang, Z., Harrison, O. J., Brasch, J., Shapiro, L., Honig, B., Vakhrushev, S. Y., Clausen, H., and Halim, A. (2017) Mammalian *O*-mannosylation of cadherins and plexins is independent of protein *O*-mannosyltransferases 1 and 2. *J. Biol. Chem.* **292,** 11586–11598 CrossRef Medline
65. Joshi, H. J., Jørgensen, A., Schjoldager, K. T., Halim, A., Dworkin, L. A., Steentoft, C., Wandall, H. H., Clausen, H., and Vakhrushev, S. Y. (2018) GlycoDomainViewer: a bioinformatics tool for contextual exploration of glycoproteomes. *Glycobiology* **28,** 131–136 CrossRef Medline
66. Hunter, I., Rehfeld, J. F., and Goetze, J. P. (2011) Measurement of the total proANP product in mammals by processing independent analysis. *J. Immunol. Methods* **370,** 104–110 CrossRef Medline

Discovery of *O*-glycans on atrial natriuretic peptide (ANP) that affect both its proteolytic degradation and potency at its cognate receptor

Lasse H. Hansen, Thomas Daugbjerg Madsen, Christoffer K. Goth, Henrik Clausen, Yang Chen, Nina Dzhoyashvili, Seethalakshmi R. Iyer, S. Jeson Sangaralingham, John C. Burnett Jr., Jens F. Rehfeld, Sergey Y. Vakhrushev, Katrine T. Schjoldager and Jens P. Goetze

J. Biol. Chem. 2019, 294:12567-12578.
doi: 10.1074/jbc.RA119.008102 originally published online June 11, 2019
